Power-Law Time-Scale Contrast for Abrupt Change Detection in Multiplicative Noise

Marie CHABERT and Jean-Yves TOURNERET
ENSEEIHT/GAPSE 2, rue Camichel BP7122, 31071 Toulouse, France
chabert@len7.enseeiht.fr

ABSTRACT

This paper addresses the problem of AC detection in multiplicative noise using the Continuous Wavelet Transform (CWT) and possible non-linear pre-processing. The quadratic pre-processing is shown to improve the performance of signature-based time-scale detectors under specific conditions on noise and signal parameters.

1 Introduction

Object contour extraction and signal segmentation require the detection and estimation of Abrupt Changes (AC) in the observed process statistics [1]. This paper addresses the problem of AC detection in multiplicative noise using the Continuous Wavelet Transform (CWT) and possible non-linear pre-processing. Multiplicative noise models have been considered in many applications. These applications include Synthetic Aperture Radar (SAR) image processing, where the reflectivity is corrupted by multiplicative speckle noise [2]. The use of the Continuous Wavelet Transform (CWT) for AC detection was motivated in [6], [3]. An interesting CWT property is a time-scale AC signature emerging from the transformed noise as scale increases. Based on this property, suboptimal time-scale detectors obtained by linear or non-linear CWT post-processings were studied. Among these detectors, the sum along scales of the CWT has received particular attention in [3]. The paper studies the influence of a non-linear pre-processing on the performance of this time-scale detector. The class of non-linear memoryless power-law transformations is considered. Such non-linearities can be justified by the fact that most functions can be approximated by a polynomial according to the well-known Weierstrass theorem ([9] p.399). The main contribution of the paper is to show that the AC detection can be improved by a non-linear preprocessing depending on noise distribution and signal parameters. A time-scale contrast is defined to decide whether pre-processing improves AC detection or not. Receiver Operational Characteristic (ROC) curves obtained with Monte-Carlo simulations are shown to be in good agreement with this time-scale contrast.

The paper is organized as follows: section 2 formulates the AC detection problem as a binary hypothesis testing problem. Section 3 studies CWT first and second order moments with possible preprocessing. Conditions under which non-linear pre-processing improves time-scale contrast are derived. Section 4 is devoted to simulation results. ROC curves show the influence of the non-linear preprocessing on suboptimal time-scale detection. Conclusions are reported in section 5.

2 Problem formulation

Consider $x(t)$ a white multiplicative noise with mean $m_x \neq 0$ and power spectral density N_x (the multiplicative noise is non zero-mean in SAR image processing [2]). The AC occurring at time t_0 denoted $s(t)$ is modelled as follows:

$$\begin{aligned} s(t) &= m_1 + (m_2 - m_1)\, U(t - t_0) \\ t &\in \Omega,\ t_0 \in \Omega,\ m_2 \geq m_1 \geq 0 \end{aligned}$$

where m_1 (respectively m_2) is the noise-free signal amplitude before (respectively after) the AC and $U(t)$ is the Heaviside function. The AC detection problem can be expressed as a simple binary hypothesis testing:

$$\begin{array}{ll} \text{Hypothesis } H_0: & y(t) = x(t) \\ \text{Hypothesis } H_1: & y(t) = x(t)s(t) \end{array} \qquad \text{(I)}$$

where the additive sensor noise is neglected as in [5]. The Neyman-Pearson detector for problem (I) is optimal in the sense that it maximizes the Probability of Detection (PD) for a fixed Probability of False Alarm (PFA). However, optimal detection requires knowledge of the observed process distribution, which may be partially known or too complex to derive. In such cases, suboptimal detectors can be studied. This paper proposes to study non-linear wavelet-based detectors as an alternative to statistical methods.

3 Time-scale analysis

The CWT of $y(t)$ is defined by:

$$C_y(a,\tau) = a^{-1/2} \int_{-\infty}^{+\infty} y(t) \psi^* \left(\frac{t-\tau}{a} \right) dt$$

where ψ is the mother wavelet, $a \in \mathbb{R}^{+*}$ is the dilation parameter and $\tau \in \mathbb{R}$ is the translation parameter. The admissibility condition (which can be expressed as $\int_{-\infty}^{+\infty} \psi(t)dt = 0$ when the Fourier transform of ψ is continuous [4]), allows to define an AC signature. This study is restricted to real admissible normalized wavelets with symmetrical bounded support $\left[\frac{-\Delta t}{2}, \frac{\Delta t}{2}\right]$.

3.1 CWT Moments

Denote $m_{n,i}(a,\tau)$ the mean of $C_{y^n}(a,\tau)$ under hypothesis H_i, $i = 0, 1$. The admissibility condition yields:

$$m_{n,0}(a,\tau) = m_{x^n} \int_{-\infty}^{+\infty} \psi^*_{a,\tau}(t)\, dt = 0$$

The CWT is invariant with respect to translations and dilations of the original signal. This property allows to define an AC signature as the mean of $C_{y^i}(a,\tau)$ under hypothesis H_1 [3]:

$$m_{n,1}(a,\tau) = \sqrt{a} I_\psi \left(\frac{t_0 - \tau}{a}\right) m_{x^n} m_1^n \left(\gamma_{21}^n - 1\right) \quad (1)$$

where $I_\psi(t) = \int_t^{+\infty} \psi^*(u)\, du$ and $\gamma_{21} = \frac{m_2}{m_1}$. The signature is conic and points to the AC instant t_0. The variance of $C_{y^n}(a,\tau)$ under hypothesis H_i denoted $\sigma^2_{n,i}(a,\tau)$ expresses as:

$$H_0 : \sigma^2_{n,0}(a,\tau) = N_{x^n}$$

$$H_1 : \sigma^2_{n,1}(a,\tau) = N_{x^n} m_1^{2n} \left(1 + \left(\gamma_{21}^{2n} - 1\right)\ J_\psi\left(\frac{t_0 - \tau}{a}\right)\right)$$

where $J_\psi(t) = \int_t^{\frac{\Delta t}{2}} |\psi(u)|^2\, du$. As an example, consider a multiplicative white noise with power spectral density $N_x = 1$ and mean $m_x = 1$. The AC parameters are $t_0 = 500$, $m_1 = 1$ and $m_2 = 1.4$. The CWT is computed for integer scales varying from 200 to 350 with the symmetrical Haar wavelet. Fig. 1 shows the ideal time-scale signature without non-linear pre-processing. The signature cross-sections (corresponding to fixed scales) are proportional to the wavelet integral (i.e. triangular cross-section for the symmetrical Haar wavelet). Fig. 2 represents the noisy CWT of $y(t)$. The conic signature is pointing to the AC instant $t_0 = 500$. Note that the signature emerges from noise for large scales. Similar time-scale signatures are obtained with power-law pre-processing. However, different signature amplitudes and time-scale noise variances are obtained [10].

3.2 Time–Scale Contrast

The complementary deflection [8] is a well-matched contrast for AC detection in multiplicative noise [3]. Under hypothesis H_1, this contrast is a time-scale signature to noise ratio for a given non-linear preprocessing. Denote $\beta_n(a,\tau)$ the complementary deflection obtained for $C_{y^n}(a,\tau)$:

$$\beta_n(a,\tau) = \frac{\left[m_{n,1}(a,\tau) - m_{n,0}(a,\tau) \mid H_0\right]^2}{\sigma^2_{n,1}(a,\tau)}$$

Straightforward computations yield:

$$\beta_n(a,\tau) = aF_x.G_{\psi,s}$$

$$\text{with} : \begin{cases} F_x = \gamma_{x^n} = \frac{m_{x^n}^2}{N_{x^n}} \\ G_s^\psi = \frac{(\gamma_{21}^n - 1)^2 \left|I_\psi\left(\frac{t_0-\tau}{a}\right)\right|^2}{1 + \left(\gamma_{21}^n - 1\right) J_\psi\left(\frac{t_0-\tau}{a}\right)} \end{cases}$$

This contrast is proportional to the scale on every line of the time-scale domain defined by $\frac{t_0-\tau}{a} = cste$. This highlights the interest of working in the time-scale domain, specially for high scales. Moreover, the time-scale contrast expresses as the product of a noise dependent term F_x and a signal and wavelet dependent term G_s^ψ. The wavelet dependence can be studied [3]. An optimal wavelet, maximizing the contrast, can be derived in the set of normalized and admissible wavelets. The optimal wavelet can be approached by the symmetrical Haar wavelet with bounded support $\left[-\frac{\Delta t}{2}, \frac{\Delta t}{2}\right]$, for small AC amplitudes [3]. Linear and non-linear contrasts are compared on the CWT maxima curve ($\tau = t_0$) using the symmetrical Haar wavelet. The noise dependent factor can be studied as a function of n for different noise distributions. In SAR image processing applications, the speckle noise is usually modelled either as a Gamma distributed noise or a Gaussian noise [2], [5].

- **Gamma Distribution**:

γ_{x^n} can be expressed as a function of $\gamma_x = \frac{m_x^2}{N_x}$ ([7], p. 116):

$$\gamma_{x^n} = \left(\frac{(\gamma_x + 2n - 1)!\,(\gamma_x - 1)!}{(\gamma_x + n - 1)!^2} - 1\right)^{-1}$$

- **Gaussian Distribution**:

γ_{x^n} expresses as ([7], p. 110):

$$\gamma_{x^n} = \left(\frac{\sum_{k=0}^{n} C_{2k}^{2n} (2k-1)!!\, \gamma_x^{-k}}{\left(\sum_{k=0}^{n/2} C_{2k}^{n} (2k-1)!!\, \gamma_x^{-k}\right)^2} - 1\right)^{-1}$$

$$\text{where } (2k-1)!! = 1.3.... (2k-1)$$

For both distributions, the contrast expresses as a function of n, γ_x and γ_{12}. Next section studies a relative efficiency to quantify the influence of a given power-law preprocessing on time-scale contrast as a function of γ_x and γ_{12}.

3.3 Relative efficiency

The relative efficiency of a nonlinear preprocessing can be defined as:

$$\rho_{n,1} = \frac{\beta_n(a,t_0)}{\beta_1(a,t_0)} = \frac{\gamma_{x^n}}{\gamma_x} \left(\frac{\gamma_{21}^n - 1}{\gamma_{21} - 1}\right)^2 \frac{\gamma_{21}^2 + 1}{\gamma_{21}^{2n} + 1} \quad (2)$$

Fig. 3 and 4 display $log(\rho_{n,1})$ for different values of n as functions of γ_{21} and γ_x for Gamma and Gaussian noise respectively.

- **Gamma Distribution**: Fig. 3 shows that power-law preprocessing does not improve the time-scale contrast for Gamma distributed noise.

- **Gaussian Distribution**: On the contrary, Fig.4 shows that, for a fixed n, the ratio $\rho_{n,1}$ is a decreasing function of γ_{21} and γ_x. Consequently, the smaller the AC amplitude, the smaller γ_x, the greater the interest of a preprocessing. Moreover, for small values of γ_{21} and γ_x, the quadratic preprocessing outperforms considerably any power-law based preprocessing. Fig. 5 displays regions of contrast improvement for different values of n for Gaussian noise.

4 Time-scale detection

Post-processing of the CWT was used in [3] to build suboptimal detectors. This paper focuses on the sum along fixed scales of the CWT denoted $D(\tau)$ which yields the following AC detection strategy:

$$H_0 \text{ accepted if } D(\tau) = \sum_{i=1}^{ns} C_{y^n}(a_i, \tau) < S(PFA) \quad \forall \tau \tag{3}$$

where ns is the number of scales and $S(PFA)$ a threshold depending on the probability of false alarm (PFA). The summation must cover several octaves in scale to sum decorrelated coefficients. In this case, the test statistics is asymptotically Gaussian according to the central limit theorem. Consequently, the threshold can be determined independently of the multiplicative noise distribution. Fig.'s 6, 7 and 8 display ROC curves (i.e. PD as function of PFA) for different values of n and Gamma and Gaussian noise.

- **Gamma Distribution**: For Gamma distributed noise, the linear detector outperforms the non-linear detectors as suggested by the time scale contrast analysis.

- **Gaussian Distribution**: On the contrary, for Gaussian noise, the detection performance clearly improves when using a non-linear pre-processing (Fig. 7) and specially for small values of γ_{21} and γ_x (Fig. 8).

5 Conclusions

The main contribution of the paper is to study the influence of nonlinear preprocessing on time-scale AC detection for signals corrupted by multiplicative noise. An appropriate time-scale contrast showed that a non-linear processing can improve the detection performance, under appropriate conditions regarding the noise distribution and signal parameters. Finally, these results were illustrated by Receiver Operating Characteristics curves for an appropriate suboptimal time-scale detector. For Gaussian noise and small values of the AC amplitude, the quadratic preprocessing is shown to outperform any power-law based preprocessing.

References

[1] M. Basseville and I. V. Nikiforov, Detection of Abrupt Changes: Theory and Application. Prentice-Hall, 1993.

[2] A. C. Bovik, "On detecting Edges in Speckle Imagery," IEEE Trans. A.S.S.P., vol. 36, n°10, 0ct. 1988.

[3] M. Chabert, J-Y. Tourneret and F. Castanié, "Time-Scale Analysis of Abrupt Changes corrupted by Multiplicative noise," Signal Processing, March 2000, vol. 80 issue 3, pp. 397-411.

[4] I. Daubechies, Ten Lectures on Wavelets, CBMS-NSF Regional Conference Series In applied Mathematics, 1992.

[5] V. Frost, J. A. Stiles, K.S. Shanmugan and J.C. Holtzman, "A model for Radar Images and Its Application to Adaptive Digital Filtering of Multiplicative Noise," IEEE Trans. on Pattern Analysis and Machine Intelligence, Vol. PAMI-4, n°2, March 1992.

[6] A. Grossmann, R. Kronland-Martinet and J. Morlet, "Reading and Understanding Continuous Wavelet Transforms," Wavelets Time-Frequency Methods and Phase Space, J.M. Combes, A. Grossmann, Ph. Tchamitchian (Eds), Springer Verlag, pp. 2-20, 1990.

[7] A. Papoulis, Probability, Random Variables and Stochastic Processes, McGraw-Hill, New york, 1991.

[8] B. Picinbono and P. Duvaut, "Detection and Contrast," Stochastic Processes in Underwater Acoustics, Lecture Notes in Control and Information Sciences (vol 85), Baker CR et Al (Eds), 1986.

[9] B. Porat, Digital Processing of Random Signals Theory and Methods, Prentice Hall Information and System Sciences Series, 1994.

[10] M. Chabert, Détection et estimation de ruptures noyées dans un bruit multiplicatif - Approches classiques et temps-échelle, these de doctorat de l'INP de Toulouse, n°1395, Décembre 1997.

[11] H. L. Van Trees, Detection, Estimation, and Modulation Theory, John Wiley & Sons, 1968.

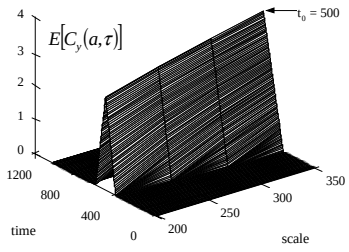

Fig.1: Step signature $(\gamma_{21} = 1.4, t_0 = 500)$ (symmetrical Haar wavelet)

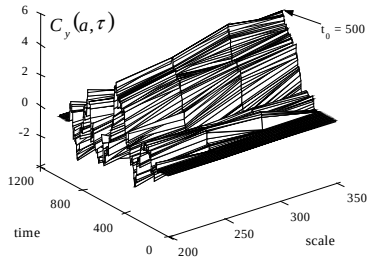

Fig.2: CWT of a step $(\gamma_{21} = 1.4, t_0 = 500)$ in Gaussian multiplicative noise $(N_x = 1)$ (symmetrical Haar wavelet)

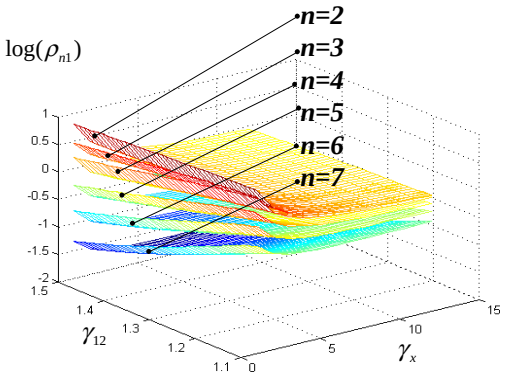

Fig.3: Relative efficiency $\rho_{n,1}$ as a function of γ_{21} and γ_x - Gaussian noise

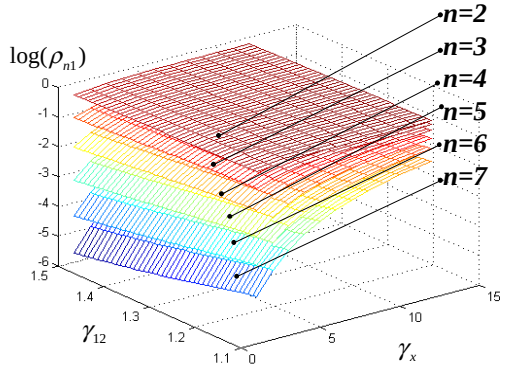

Fig.4: Relative efficiency $\rho_{n,1}$ as a function of γ_{21} and γ_x - Gamma distributed noise

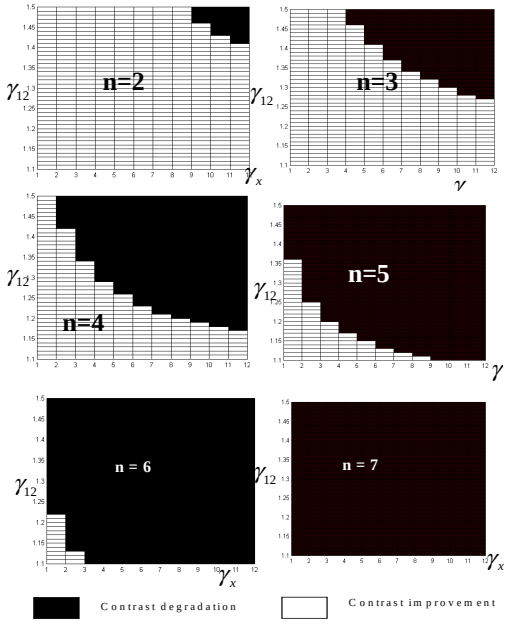

Fig.5: Regions of contrast improvement as a function of γ_{21} and γ_x - Gaussian noise

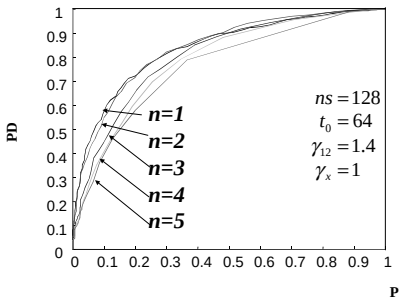

Fig.6: ROC curves of D as functions of n- Gamma distributed noise

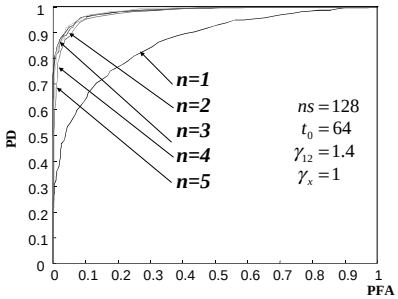

Fig.7: ROC curves of D as functions of n- Gaussian noise

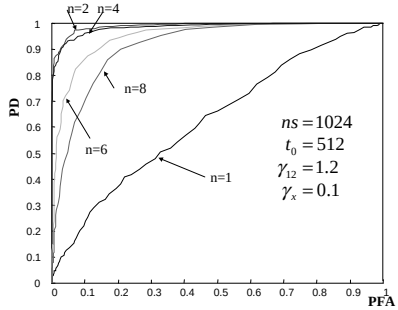

Fig.8: ROC curves of D as functions of n- Gaussian noise